Available online at www.sciencedirect.com
ScienceDirect
Journal of Power Sources 160 (2006) 529–535
JOURNAL OF POWER SOURCES
www.elsevier.com/locate/jpowsour

Combustion synthesis of nanocrystalline $LiNi_YCo_{1-2Y}Mn_{1+Y}O_4$ spinels for 5 V cathode materials Characterization and electrochemical properties

R.M. Rojas [a,*], J.M. Amarilla [a], L. Pascual [a], J.M. Rojo [a], D. Kovacheva [b], K. Petrov [b]

[a] *Instituto de Ciencia de Materiales de Madrid, Consejo Superior de Investigaciones Científicas, Sor Juana Inés de la Cruz no. 3, Cantoblanco, 28049 Madrid, Spain*
[b] *Institute of General and Inorganic Chemistry, Bulgarian Academy of Sciences, 1113 Sofia, Bulgaria*

Received 16 November 2005; received in revised form 4 January 2006; accepted 4 January 2006
Available online 9 February 2006

Abstract

Nanosized double substituted $LiNi_YCo_{1-2Y}Mn_{1+Y}O_4$ ($Y = 0.05$, 0.1, 0.25 and 0.45) spinels have been synthesized by a single-step combustion-aided procedure, which use sucrose as fuel. The as prepared samples contained some amorphous organic impurities that were removed after a short heating at 400 °C. The samples have been characterized by X-ray diffraction, thermal analysis and transmission electron microscopy. Lattice parameter of the spinels increased with nickel content, and decreased from 400 to 600 °C, at which temperature stoichiometric spinels with particle size of ≈20 nm were obtained. The electrochemical properties of the 600 °C-treated samples in the 5 V region have been studied. The sample with composition $LiNi_{0.45}Co_{0.1}Mn_{1.45}O_4$ has shown the best electrochemical performance, with redox potential of 4.6 V, capacity of 129.6 mAh g^{-1}, cyclability of 99.6% per cycle, and retained the capacity up to 1*C* rate.

Keywords: Lithium batteries; $LiMn_2O_4$; Spinel; Cathode materials; 5 V electrodes

1. Introduction

Recent trends in Li-ion batteries are focused on the development and characterization of high-voltage cathode materials working in the 5 V region [1]. It has been shown that when manganese atoms are substituted in the spinel-type $LiMn_2O_4$ oxide by other transition metals giving way to the $LiM_YMn_{2-Y}O_4$ (M = Cr, Ni, Co, Al, Fe, Cu, Mg, etc.) compounds, improvement of cyclability is achieved [2–6]. For some particular dopant cations and for large dopant contents, a large part of the cathode capacity is observed at potentials between 4.7 and 5.2 V. As Mn^{4+} ions are electrochemically inactive in these compounds at these potentials, the shift of the main reversible redox process from about 4 to nearly 5 V during Li^+ insertion/extraction has been attributed to the redox reaction of the substituting transition metals [7–12]. Simultaneous partial replacement of manganese by two transition metals has also been reported [13–20], and it has been pointed out that this co-doping has a synergistic effect on the improvement of the cycling life of these materials as cathodes in lithium batteries [14,19].

It is well known that the electrochemical behavior of the cathode materials depends not only on the composition of the spinel phase, but also on its morphology and defect structure. These parameters are determined by the synthesis procedure and the thermal treatment conditions. Recently, we have shown that materials obtained by the combustion route with sucrose as fuel and treated at relatively low temperature, lead to spinels with nanosize particles with very good electrochemical performance, particularly at high current density [21–23]. Aimed to influence the voltage of the 5 V region, and to improve the rate capability of the materials, we have carried out the synthesis of the double substituted $LiNi_YCo_{1-2Y}Mn_{1+Y}O_4$ ($Y = 0.45$, 0.25, 0.1 and 0.05) spinels by the sucrose-aided combustion method. To guarantee the electrochemical activity in the 5 V region the amounts

* Corresponding author. Tel.: +34 91 334 90 73; fax: +34 91 372 06 23.
E-mail address: rmrojas@icmm.csic.es (R.M. Rojas).

0378-7753/$ – see front matter © 2006 Elsevier B.V. All rights reserved.
doi:10.1016/j.jpowsour.2006.01.012

of Ni and Co dopants were chosen to keep the oxidation state of manganese in the spinels as Mn^{4+}. The samples have been characterized by X-ray diffraction, thermal analysis and electron microscopy. The electrochemical behavior of the spinels synthesized has been studied, and compared with the reported for the end members compounds $LiNi_{0.5}Mn_{1.5}O_4$ and $LiCoMnO_4$.

2. Experimental

The $LiNi_YCo_{1-2Y}Mn_{1+Y}O_4$ ($Y = 0.05$, 0.1, 0.25 and 0.45) spinels were synthesized by the combustion method, from the stoichiometric amounts of Li, Ni, Co and Mn nitrates, which act as the oxidants, and sucrose as fuel. The reaction can be described as follows:

$$LiNO_3 + YNi(NO_3)_2 \cdot 4H_2O + (1-2Y)Co(NO_3)_2 \cdot 6H_2O + (1+Y)Mn(NO_3)_2 \cdot 4H_2O + \tfrac{1}{2}C_{12}H_{22}O_{11} + \tfrac{1}{2}O_2 \rightarrow LiNi_YCo_{1-2Y}Mn_{1+Y}O_4 + 6CO_2 + (\tfrac{31}{2} - 4Y)H_2O + \tfrac{5}{2}N_2$$

When using the stoichiometric amount of sucrose, i.e. 1/2 mol of $C_{12}H_{22}O_{11}$, that keeps the oxidant/fuel ratio = 1:1 [24,25], the reaction is extremely violent. To avoid it, and after a detailed examination of the combustion process, the oxidant/fuel ratio chosen was ≈0.5, i.e. 1 mol $C_{12}H_{22}O_{11}$. In this way the reaction can be easily controlled. It is worth to mention that the synthesis method chosen allows a simple way of controlling the reaction intensity, and makes it very appropriated for preparation of nanosize materials with a variety of compositions. The reagents solution was heated at about 120 °C for 30 min, and when dried it starts to swell up due to the evolution of gases generated in the thermolysis of the reagents, giving way to a foamy mass. After a few minutes, the mass starts to burn up spontaneously without flame. The product of the reaction is a very light and downy black powder. The yield is ≈98%. Samples once obtained were heated at 400 °C for 1 h. These samples will be hereafter referred to as "as prepared". They were then accumulatively treated in air at 400 °C and at 600 °C for 6 h, at a heating/cooling rate of 2 °C min^{-1}.

The phase purity and morphology of the samples were studied by X-ray powder diffraction. X-ray powder diffraction patterns were recorded at room temperature in a Bruker D8 diffractometer, with Cu Kα radiation. The patterns were obtained in the step scanning mode at 0.04° (2θ) step and 2 s $step^{-1}$ counting time, within the range $10° \leq 2\theta \leq 80°$. Lattice parameters were refined with the CELREF program [26]. The average crystallite size was calculated from several diffraction lines from the Scherrer formula:

$$D = \frac{\lambda}{\beta}\cos\theta$$

λ is the wavelength of Cu Kα = 1.54186 Å, θ the diffraction angle, and $\beta = \sqrt{(\beta_m^2 - \beta_s^2)}$ is the corrected half-width of the diffraction peaks, where β_m is the observed half-width of the experimental diffraction peaks and β_s is the half-width of the diffraction peaks of a standard sample, in our case the $Y = 0.45$ sample heated at 1000 °C.

Transmission electron micrographs were taken in a JEOL 2000FX electron microscope operating at an acceleration voltage of 200 kV. The samples were dispersed in *n*-butyl alcohol, and drops of the dispersion were transferred to a holey carbon-coated copper grid.

Differential (DTA) and thermogravimetric (TG) analysis were carried out simultaneously with a DTA/TG Seiko 320U instrument up to 1000 °C in still air, and 10 °C min^{-1} heating and cooling rates. About 50 mg of sample was used in each run, and α-Al_2O_3 was the inert reference.

The study of the electrochemical behavior of the $LiNi_YCo_{1-2Y}Mn_{1+Y}O_4$ spinels heated at 600 °C for 6 h was performed in a Swagelok® two-electrode lithium cell. Positive electrode composites were prepared from the spinel powder (≈20 mg or 72 wt.%), MMM Super P carbon black (17 wt.%) and polyvinylidenefluoride (PVDF, 11 wt.%). These percentages were chosen in accordance with those reported in Ref. [27]. We proceeded as follows: *N*-methylpyrrolidinone (1 ml per gram of PVDF) was added to the mixture of the three components, and they were stirred overnight. The solvent was evaporated at 80 °C. Then cylindrical pellets (12 mm diameter and ca. 0.2 mm thickness) of positive electrode were obtained after cold pressing at 370 MPa. The negative electrode was a lithium foil, which also operated as reference electrode. The electrodes were separated by a Whatman BSF80 paper soaked in the electrolyte, which was a 1 M solution of $LiPF_6$ in ethylene carbonate and dimethyl carbonate as supplied by Merck. The components were assembled into a two-electrode Swagelok® cell within an argon glove box in which water content was kept below 1 ppm. The cell was galvanostatically cycled at room temperature in the voltage range of 3.4–5.2 V at 0.5*C* rate in charge and at *C* rate in discharge with an Arbin battery tester system (BT2043). Rate capability of $LiNi_{0.45}Co_{0.1}Mn_{1.45}O_4$ was studied by cycling the test cell at increasing discharge currents from 0.5 to 14*C* rate between 3.4 and 5.2 V at 25 ± 0.2 °C. Every charge was carried out at 0.5*C* rate. *C* is the capacity of the cathode calculated from the theoretical capacity of the $LiNi_YCo_{1-2Y}Mn_{1+Y}O_4$ spinel and the mass of spinel used in the composite. The *C* coefficients are the inverse of the theoretical charge/discharge time.

3. Results and discussion

3.1. Structural, thermal and morphological characterization

The X-ray patterns obtained for the "as prepared" samples are presented in Fig. 1. They show broad diffraction lines, which can be fully indexed in the *Fd*3*m* space group. There is a shift of the diffraction peaks towards higher 2θ angles with decreasing the Ni-content, indicating the progressive diminution of lattice parameter of the "as prepared" samples on decreasing the Ni doping. Lattice parameter values go from $a = 8.184(4)$ Å for the sample at $Y = 0.45$ to 8.101(7) Å for the sample at $Y = 0.05$. The X-ray patterns of all samples show the (2 2 0) diffraction line, which even having a very low intensity is not negligible. It indicates the presence of some heavy cations in the tetrahedral

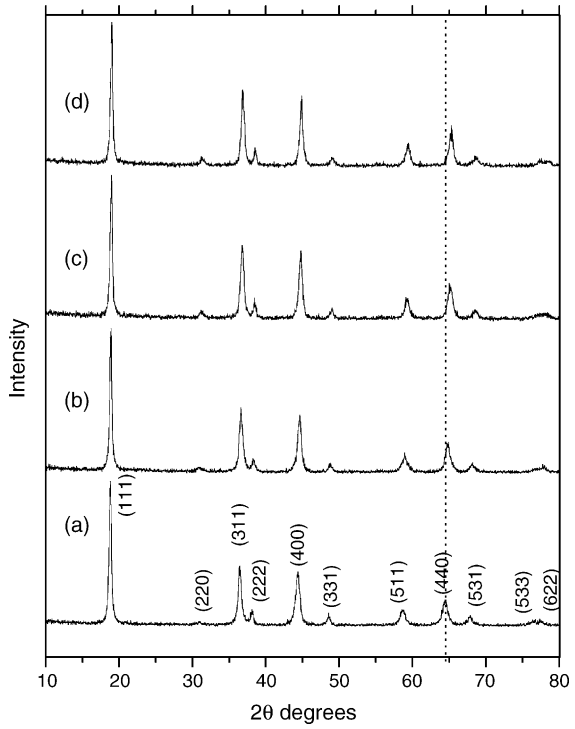

Fig. 1. X-ray diffraction patters of the "as prepared" samples: (a) $LiNi_{0.45}Co_{0.1}Mn_{1.45}O_4$, (b) $LiNi_{0.25}Co_{0.5}Mn_{1.25}O_4$, (c) $LiNi_{0.1}Co_{0.8}Mn_{1.1}O_4$ and (d) $LiNi_{0.05}Co_{0.9}Mn_{1.05}O_4$.

positions of the spinel structure. This peak is more pronounced for the Co-rich samples, i.e. $Y = 0.1$ and 0.05.

Thermal analysis curves recorded for all the "as prepared" samples are similar. As an example, DTA and TG curves recorded simultaneously for the sample at $Y = 0.45$ are presented in Fig. 2. An exothermic peak and a step are observed in the DTA and TG curves, respectively, at about 200 °C. Both effects can be ascribed to the combustion of some organic amorphous impurities [22,23]. These impurities are not detectable by X-ray diffraction, and indicate that the "as prepared" samples are not pure spinels. They have some organic residues, which disappear after heating of the samples at 400 °C for 6 h. This temperature

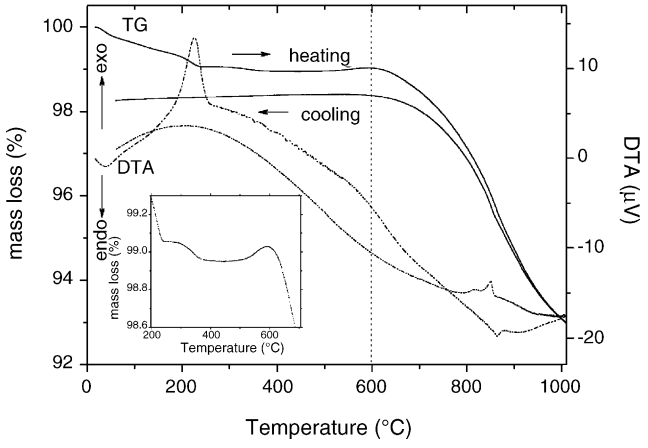

Fig. 2. DTA/TG curves recorded for the "as prepared" $LiNi_{0.45}Co_{0.1}Mn_{1.45}O_4$ spinel. The inset shows the enlarged TG curve in the 200–700 °C region.

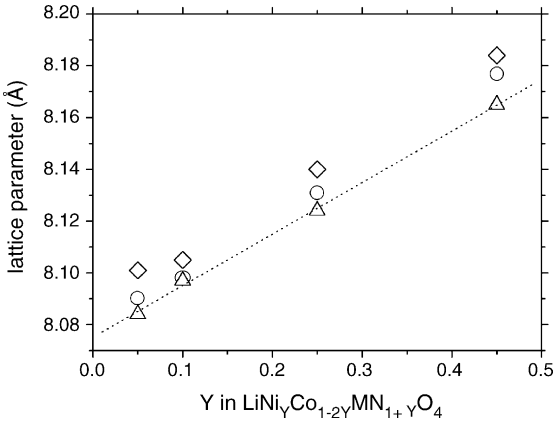

Fig. 3. Variation of the lattice parameter of the $LiNi_YCo_{1-2Y}Mn_{1+Y}O_4$ samples "as prepared" (◊), heated at 400 °C (◯) and at 600 °C (△) for 6 h (dotted line corresponds to the linear fit).

was chosen because it corresponds to the lowest temperature of the plateau appearing in the TG curve between 400 and 500 °C (Fig. 2). In effect, DTA and TG curves recorded for the samples after the latter thermal treatment do not show either the exothermic effect or the step already mentioned. Between 500 and 600 °C the sample undergoes a weight gain (Fig. 2, inset). For temperatures higher than 600 °C the decomposition of the spinel starts off, and a continuous weight loss takes place up to 1000 °C. This weight loss is ascribed to oxygen removal [22,23]. The TG curve recorded on cooling indicates that the mass lost on heating is not completely regained on cooling.

Having in mind the results of thermal analysis we decided to heat the "as prepared" samples at 400 and 600 °C for 6 h. The evolution of the lattice parameter with composition for these two temperatures is shown in Fig. 3, and the values determined are summarized in Table 1. It is observed that for all compositions the lattice parameter decreases from the samples "as prepared", i.e. heated at 400 °C for 1 h, to the samples heated at 600 °C for 6 h, i.e. with increasing the temperature of the thermal treatment. Such behavior is unusual, since an increase of the lattice parameter with temperature has been generally reported [17,22]. The variation of the lattice parameters with temperature (Fig. 3) can be related to the specific conditions of the method of synthesis. At the first stages of the reaction, during the swelling process, a local reducing atmosphere is generated due to the thermolysis of the reagents. In these conditions some cations could have oxidation states lower than the theoretical ones for spinels. Reduction processes have been also reported for the thermal decomposition of some organic salts [28,29]. Upon heating the samples at 400 °C for 6 h, besides purification of the samples, some oxidation of the spinels takes place, and they become fully oxidized after thermal treatment at 600 °C for 6 h. The oxidation process is clearly observable in the TG curve recorded for the $Y = 0.45$ sample (Fig. 2, inset) where a weight gain is seen in the 500–600 °C range. This oxidation process can account for the observed diminution of lattice parameters along the thermal treatments. A similar diminution of the lattice parameters between 300 and 600 °C has been reported for the $LiNi_{0.5}Mn_{1.5}O_4$ synthesized by a sol–gel procedure [8].

Table 1
Structural and electrochemical data for the $LiNi_YCo_{1-2Y}Mn_{1+Y}O_4$ spinels

Sample	Treatment temperature (°C)[a]	Lattice parameter (Å)	Particle size[b] (nm)	Capacity at the 1st discharge cycle (mAh g^{-1})	Capacity at the 50th discharge cycle (mAh g^{-1})
$LiNi_{0.45}Co_{0.1}Mn_{1.45}O_4$	As prepared	8.184(4)	15		
	400	8.177(2)	16		
	600	8.165(1)	25	129.6	104.6
$LiNi_{0.25}Co_{0.5}Mn_{1.25}O_4$	As prepared	8.140(2)	14		
	400	8.131(3)	16		
	600	8.124(2)	20	105.6	65.6
$LiNi_{0.1}Co_{0.8}Mn_{1.1}O_4$	As prepared	8.105(3)	16		
	400	8.098(3)	16		
	600	8.097(2)	21	88.9	39.3
$LiNi_{0.05}Co_{0.9}Mn_{1.05}O_4$	As prepared	8.101(7)	16		
	400	8.090(3)	19		
	600	8.084(2)	24	77.8	19.2

[a] The samples were heated for 6 h at the temperatures indicated.
[b] From X-ray diffraction patterns.

On increasing the Ni-content lattice parameter of the double substituted spinels linearly increases either for the "as prepared" or for the heat-treated samples (Fig. 3). This linear increase of the cubic parameter indicates the formation of a solid solution in the whole compositional interval. Moreover, the lattice parameter values range between the reported for the end-members of the solid solution, i.e. $LiCoMnO_4$ and $LiNi_{0.5}Mn_{1.5}O_4$, which are $a = 8.052$ Å [9,30] and $a = 8.1757(5)$ Å [8,22], respectively. The increase of the lattice parameter is explained considering the larger ionic radius of $^{VI}Ni^{2+}$ (0.69 Å) compared to the ionic radius of $^{VI}Co^{3+}$ (0.545 Å) [31].

The evolution of particle size with thermal treatment has also been investigated. The mean coherent domain size has been calculated from the X-ray patterns of the "as prepared" and heat-treated samples, by the Scherrer formula; and they are summarized in Table 1. A result to remark is that in all cases we are dealing with nanometric materials. The small particle size shown by the $LiNi_YCo_{1-2Y}Mn_{1+Y}O_4$ synthesized by the sucrose-aided combustion procedure can be accounted for bearing in mind the gases evolved during the combustion. They can produce a spreading out of the reaction mass separating the particles, and also can help to dissipate the heat developed during the burning and hence, inhibiting the sintering of the particles. The variation of the crystallite size with composition is negligible, and only a small increase with the temperature is observed. The "as prepared" samples have an average crystallite size of ≈14 nm, and for the 600 °C-treated samples it is of ≈20 nm. Transmission electron micrograph were also taken and as an example, a micrograph of the $Y = 0.45$ spinel heated at 600 °C for 6 h can be seen in Fig. 4a. In Fig. 4b, the corresponding particle size histogram, and the fitting to a Gaussian curve is presented. A homogeneous distribution of the faceted particles is observed, the average particle size deduced from TEM is 22 nm, with a standard deviation ±7 nm, that fairly agrees with the values determined from XRD analysis.

All the above described results and considerations lead us to conclude that 600 °C is the most appropriate temperature for obtaining the stoichiometric nanostructured double substituted Ni–Co lithium manganese spinels synthesized by the sucrose-aided combustion method. That is the reason why these are the samples whose electrochemical behavior has been investigated.

3.2. Electrochemical properties

The charge/discharge curves of the $LiNi_YCo_{1-2Y}Mn_{1+Y}O_4$ spinels registered at 0.5*C*/*C* charge/discharge rate are plotted in Fig. 5a. On increasing the nickel content, the average redox potential decreases, and the shape of the curves becomes less sloping. Thus, for the richest Ni-sample, $Y = 0.45$, the profile shows a well-defined flat plateau at ≈4.6 V. The discharge capacity notably increases on increasing the Ni-content. It rises from 77.8 mAh g^{-1} for $Y = 0.05$ to 129.7 mAh g^{-1} for $Y = 0.45$. The latter value is very close to the theoretical one, $Q_{theor} = 146.53$ mAh g^{-1}, and to values reported in the literature [17], even though we have used notably higher discharge currents. This result seems to indicate that the $LiNi_{0.45}Co_{0.1}Mn_{1.45}O_4$ has an elevated rate capability.

The lithium insertion degree, ΔLi^+, determined from the capacity drained for the cell increases as the Ni-content does. It rises from $\Delta Li^+ = 0.54$ for $Y = 0.05$ to $\Delta Li^+ = 0.88$ for $Y = 0.45$. In Fig. 5b, the variation of ΔLi^+ versus Ni-content has been plotted. The insertion degree of the $LiNi_{0.05}Co_{0.9}Mn_{1.05}O_4$, $\Delta Li^+ = 0.54$, is far greater than expected, $\Delta Li^+ = 0.1$, if only the nickel ions would be the electrochemically active. This result demonstrates that besides Ni^{2+}, the Co^{3+} is also oxidized in the explored potential region (voltage window 3.4–5.2 V). On the other hand, if both cations can be oxidized, the lithium insertion degree must be $\Delta Li^+ = 1$ for every sample. However, we observe that ΔLi^+ linearly decreases on increasing the Co-content. In our case, this decrease cannot be ascribable to kinetic limitations because the particle size is very small (≈20 nm) and it is similar for every sample. Instead, it would indicate that it is more difficult to extract/insert lithium in the Co-rich samples. It may be due to the high potential of Co^{3+}/Co^{4+} couple [6,9,30], and to the presence of some heavy atoms in tetrahedral positions, as shown by X-ray diffraction (Fig. 1).

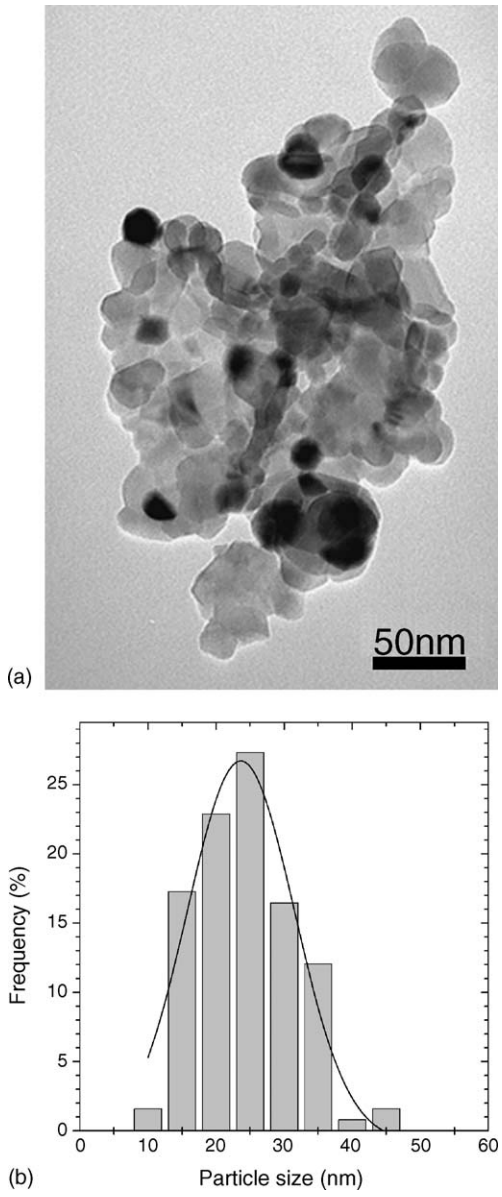

Fig. 4. TEM micrograph of: (a) the $LiNi_{0.45}Co_{0.1}Mn_{1.45}O_4$ spinel heated at 600 °C for 6 h and (b) the corresponding histogram.

To analyze the difference in the shape of the charge/discharge curves of the $LiNi_YCo_{1-2Y}Mn_{1+Y}O_4$ spinels, in Fig. 6 we have plotted the incremental derivative capacity, $\Delta Q/\Delta E$ versus voltage. For the nickel-rich $LiNi_{0.45}Co_{0.1}Mn_{1.45}O_4$ spinel, two narrow and well-resolved peaks are observed. These two peaks centered at very closed potentials, $E = 4.59$ and 4.66 V, have been associated to the $Ni^{2+} \leftrightarrow Ni^{3+}$ and $Ni^{3+} \leftrightarrow Ni^{4+}$ couples, respectively [32]. Alcántara et al. [17] have also observed two peaks during the charge of the $LiNi_{0.4}Co_{0.2}Mn_{1.4}O_4$ spinel, and by ex situ X-ray diffraction studies they ascribed these peaks to a two one-phase topotactic reaction. Some marginal redox activity is observed around 4 V, which is related to very small amounts of Mn^{3+} in the sample. For the spinel at $Y = 0.25$, the two peaks at $E \approx 4.6$ V are still observed, but they have lower intensity, and are broader than those of the sample at $Y = 0.45$. Moreover, a shoulder at higher potential, $E \approx 4.9$ V, appears. On decreasing

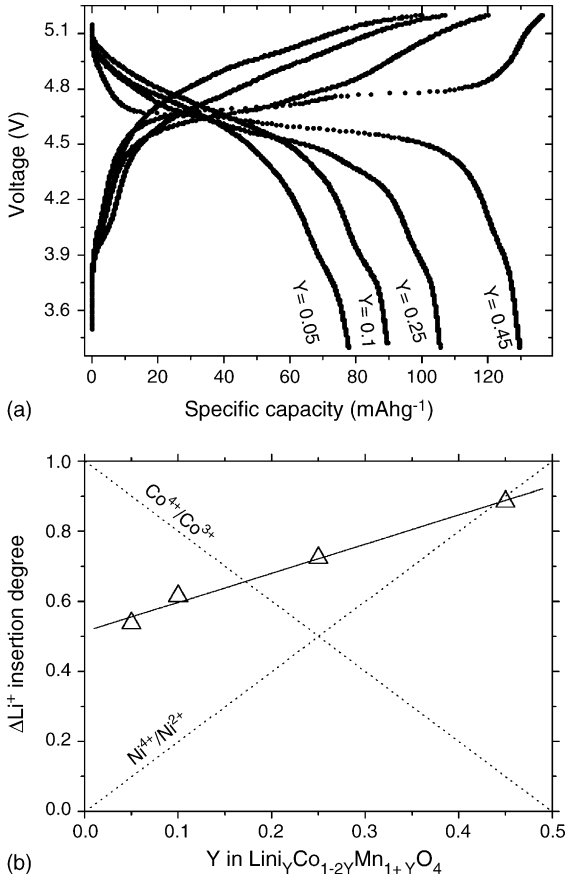

Fig. 5. Charge/discharge curves of: (a) $LiNi_YCo_{1-2Y}Mn_{1+Y}O_4$ spinels heated at 600 °C for 6 h, registered at 0.5C rate in charge and at C rate in discharge and (b) ΔLi^+ insertion degree vs. Ni-content in $LiNi_YCo_{1-2Y}Mn_{1+Y}O_4$. Solid line is a guide to the eye; dotted lines correspond to the expected ΔLi^+ assuming that only the Co^{4+}/Co^{3+}or Ni^{4+}/Ni^{2+} reactions take place.

the Ni-content, sample $Y = 0.1$, the former two peaks overlap in a broad peak at ≈4.6 V, and another new broad peak is observed at about 4.8 V. For the $Y = 0.05$ only the broad peak at ≈4.8 V is distinguished. As the Co^{3+}/Co^{4+} redox reactions take place at

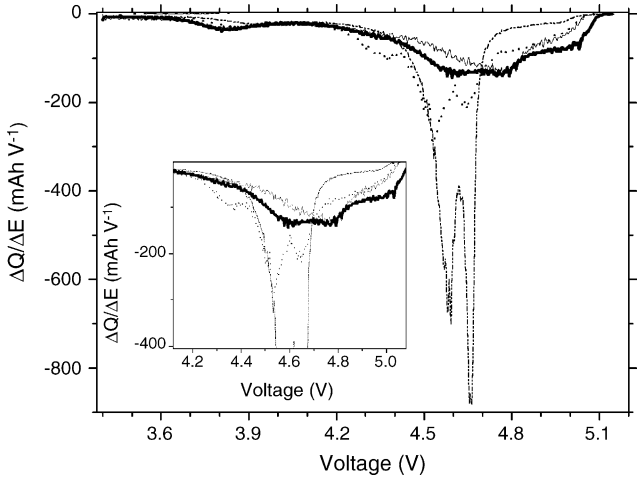

Fig. 6. Plot of $\Delta Q/\Delta E$ vs. V for the $LiNi_YCo_{1-2Y}Mn_{1+Y}O_4$ spinels heated at 600 °C for 6 h. Dash dot line, $Y = 0.45$; dot line, $Y = 0.25$; thick straight line, $Y = 0.1$ and thin straight line, $Y = 0.05$.

higher potentials than the Ni^{2+}/Ni^{4+} [6,27,30], and taking into account that our samples are active in the 5 V region, the new peaks at 4.8 V are ascribed to the former redox reaction. The sloping shapes of the curves and the increase of the average redox potentials observed for the richest Co-doped samples can be explained by the overlapping of the Ni^{2+}/Ni^{4+} and Co^{3+}/Co^{4+} reactions.

The cycling performance test of $LiNi_YCo_{1-2Y}Mn_{1+Y}O_4$ spinels has been carried out cycling the cells at 0.5*C*/*C* charge/discharge rates (voltage window of 3.4–5.2 V). As an example, in Fig. 7 a selection of charge/discharge curves recorded during cycling of the $Y=0.45$ and 0.1 spinels have been plotted. It is observed that the capacity of the $LiNi_{0.45}Co_{0.1}Mn_{1.45}O_4$ decreases smoothly from 129.7 to 104.6 mAh g^{-1} for the 50th cycle, but the capacity of the $LiNi_{0.1}Co_{0.8}Mn_{1.1}O_4$ significantly decreases from 91 to 40.6 mAh g^{-1}. This result indicates that $LiNi_{0.45}Co_{0.1}Mn_{1.45}O_4$ has a better cycling behavior that $LiNi_{0.1}Co_{0.8}Mn_{1.1}O_4$. For the latter spinel a significant drop of the redox potentials with the cycle number is observed, as well as a dramatic loss of the discharge capacity. It is worth to mention that for the samples with $Y \leq 0.25$ we have had severe difficulties on charging (Fig. 7). In fact, to complete the cycling tests and around the 20th cycle we must do the following manipulations: (i) wash inside the dry box the cathode with the electrolyte and (ii) change the electrolyte-

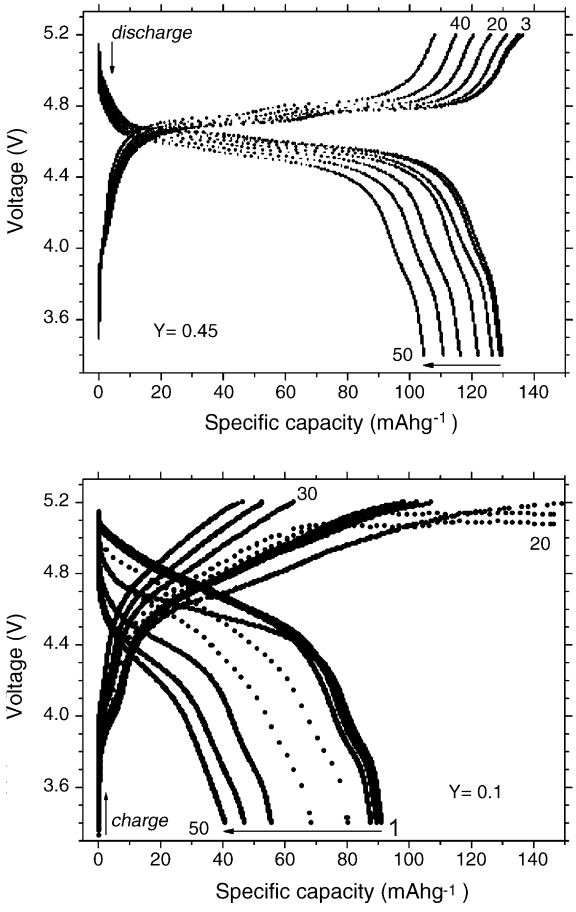

Fig. 7. Discharge curves vs. cycle number for the $LiNi_{0.45}Co_{0.1}Mn_{1.45}O_4$ ($Y=0.45$) and $LiNi_{0.1}Co_{0.9}Mn_{1.01}O_4$ ($Y=0.1$) spinels heated at 600 °C for 6 h.

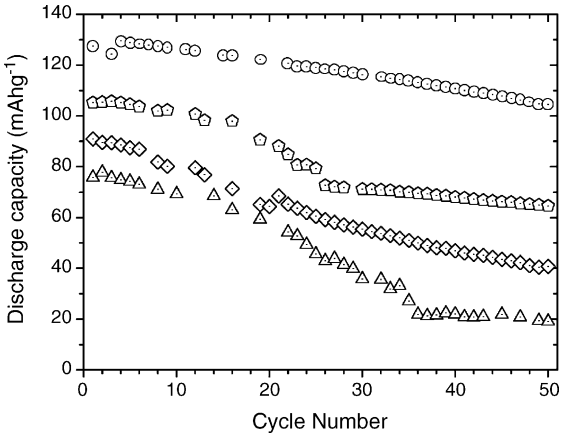

Fig. 8. Variation of the discharge capacity vs. cycle number for $LiNi_YCo_{1-2Y}Mn_{1+Y}O_4$ spinels heated at 600 °C for 6 h. (◯, $Y=0.45$; ⬠, $Y=0.25$; ◊, $Y=0.1$ and △, $Y=0.05$.)

soaked separator and the lithium foil. The re-assembled cells could be then cycled again, demonstrating that the drastic capacity loss was not caused by degradation of the spinel active material. This point was also confirmed by recording the X-ray pattern of the charged cathode after the cycling studies. The pattern was practically identical to the one recorded for the pristine material. The larger capacity values of charge compared to discharge (Fig. 5a) indicates that some degradation of the electrolyte takes place at the high anodic potential used. This degradation appears to be enhanced by increased Co-content.

The variation of the discharge capacity versus cycle number for $LiNi_YCo_{1-2Y}Mn_{1+Y}O_4$ spinels is plotted in Fig. 8. The results reveal that the cycling behavior remarkably depends on composition. On increasing the Ni-content, the capacity retention up to the 50th cycle notably rises from 24.6% for $Y=0.05$ to 80.6% for $Y=0.45$. The low capacity retention of the samples with $Y \leq 0.25$ occurs even after washing of the cathode and changing of the lithium foil and the electrolyte. The poor cycling behavior of the latter spinels shows that they are not adapted to be used in practical applications. Nevertheless, the $LiNi_{0.45}Co_{0.1}Mn_{1.45}O_4$ has a high starting capacity ($Q_{disch.}=129.6$ mAh g^{-1}) and a small capacity loss during cycling. The cyclability, determined from the slope of the fitted straight line of $Q_{disch.}$(mAh g^{-1}) versus E(V) was 99.59% per cycle. This value evidences the good reversibility of the Li^+ de-/insertion reactions in this spinel, and it is close to previously report by us for $LiNi_{0.5}Mn_{1.5}O_4$ synthesized at 800 °C by the same combustion-aided method [22] and remarkably superior to the reported for undoped $LiMn_2O_4$ [33]. The capacity of the 600 °C-treated $LiNi_{0.45}Co_{0.1}Mn_{1.45}O_4$ is higher than the reported for the $LiNi_{0.4}Co_{0.2}Mn_{1.4}O_4$ annealed at 700 °C [17], even at the fast discharge conditions used in this work.

We have analyzed the rate capability of the $LiNi_{0.45}Co_{0.1}Mn_{1.45}O_4$ heated at 600 °C between 0.5 and 14*C* discharge current. In Fig. 9, the evolution of discharge capacity versus current is displayed. It is worth to remark that the starting capacity is retained even at current as high as 1*C*. For 2*C* current, i.e. for a theoretical discharge time of only 30 min, the capacity is 111.8 mAh g^{-1}, that is 86% the

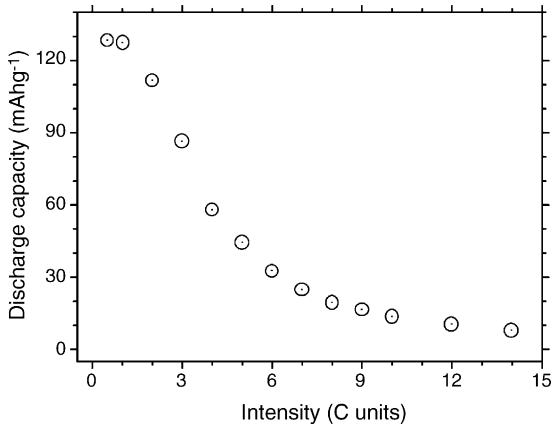

Fig. 9. Evolution of discharge capacity of the $LiNi_{0.45}Co_{0.1}Mn_{1.45}O_4$ spinel heated at 600 °C for 6 h vs. intensity current.

initial capacity. These results show the high rate capability of $LiNi_{0.45}Co_{0.1}Mn_{1.45}O_4$ that can be explained by the nanometric size of the particles of the active material synthesized by the sucrose-aided combustion method (Fig. 4). The progressive increase of the current provokes a decrease of the capacity; for 8*C* rate the capacity is 20 mAh g^{-1}.

After discharge at 14*C*, the cell was cycled again at 0.5*C* rate. At this low current, the capacity notably increases, attaining a value of $Q = 121$ mAh g^{-1}, which is very close to the starting one (Fig. 5a). This result shows that the capacity loss at very high currents is not caused by deterioration of the spinels itself, but due to kinetics limitations that are noteworthy when very fast discharge rate are used.

4. Concluding remarks

The sucrose-aided combustion method is very appropriate for the synthesis of spinel double substituted $LiNi_YCo_{1-2Y}Mn_{1+Y}O_4$ cathode materials. It is very simple, not expensive, and affords nanosized materials with good electrochemical properties. The lattice parameter of the "as prepared" spinels increases on increasing the nickel content *Y*, and decreases along the thermal treatment at 400 and 600 °C. Annealing at 600 °C for 6 h yields pure and stoichiometric spinels with ≈20 nm particle sizes. The $LiNi_{0.45}Co_{0.1}Mn_{1.45}O_4$ spinels synthesized by this method has a very high redox potential, $E = 4.6$ V, elevated capacity and specific energy, $Q = 129.6$ mAh g^{-1} and 596.2 Wh K g^{-1}, respectively; a cyclability of 99.6% per cycle, and retains the capacity up to 1*C* rate. All these characteristics make this spinel very attractive for use as positive electrode in Li-ion batteries for high power devices such as the electric vehicle.

Acknowledgements

Financial support through the projects MAT 2005-01606 (MEC), GR/MAT/0426/2004 (CAM) and the joint project CSIC-Bulgarian Academy of Sciences no. 2004BG0010 is thankfully recognized.

References

[1] H. Kawai, M. Nagata, H. Tukamoto, A.R. West, J. Power Sources 81–82 (1999) 67.
[2] C. Sigala, D. Guyomard, A. Verbaere, Y. Piffard, M. Tournoux, Solid State Ionics 81 (1995) 167.
[3] L. Guohua, H. Ikuta, T. Uchida, M. Wakihara, J. Electrochem. Soc. 143 (1996) 178.
[4] W. Liu, K. Kowal, G.C. Farrington, J. Electrochem. Soc. 143 (1996) 3590.
[5] P. Arora, B.N. Popov, R.E. White, J. Electrochem. Soc. 145 (1998) 807.
[6] J.M. Amarilla, J.L. Martín de Vidales, R.M. Rojas, Solid State Ionics 127 (2000) 73.
[7] Y. Ein-Eli, W.F. Howard Jr., J. Electrochem. Soc. 144 (1997) L205.
[8] Q. Zhong, A. Bonakdarpour, M. Zhang, Y. Gao, J.R. Dahn, J. Electrochem. Soc. 144 (1997) 205.
[9] H. Kawai, M. Nagata, H. Kageyama, H. Tukamoto, A.R. West, Electrochim. Acta 45 (1999) 315.
[10] C. Sigala, A. Le Gal La Salle, Y. Piffard, D. Guyomard, J. Electrochem. Soc. 148 (2001) A826.
[11] H. Shigemura, H. Sakaebe, H. Kageyama, H. Kobayashi, A.R. West, R. Kanno, S. Morimoto, S. Nasu, M. Tabuchi, J. Electrochem. Soc. 148 (2001) A730.
[12] H. Shigemura, M. Tabuchi, H. Kobayashi, H. Sakaebe, A. Hirano, H. Kageyama, J. Mater. Chem. 12 (2002) 1882.
[13] Y. Ein-Eli, J.T. Vaughey, M.M. Thackeray, S. Mukerjee, X.Q. Yang, J. McBreen, J. Electrochem. Soc. 146 (1999) 908.
[14] F. Bonino, S. Panero, D. Satolli, B. Scrosati, J. Power Sources 97–98 (2001) 389.
[15] K.-J. Hong, Y.-K. Sun, J. Power Sources 109 (2002) 427.
[16] B.J. Hwang, R. Santhanam, S.G. Hu, J. Power Sources 108 (2002) 250.
[17] R. Alcántara, M. Jaraba, P. Lavela, J.L. Tirado, J. Electrochem. Soc. 151 (2004) A53.
[18] R. Alcántara, M. Jaraba, P. Lavela, J.L. Tirado, Chem. Mater. 15 (2003) 1210.
[19] R. Alcántara, M. Jaraba, P. Lavela, J.M. Lloris, C. Pérez Vicente, J.L. Tirado, J. Electrochem. Soc. 152 (2005) A13.
[20] T.A. Arunkumar, A. Manthiram, Electrochim. Acta 50 (2005) 5568.
[21] D. Kovacheva, H. Gadjov, K. Petrov, S. Mandal, M.G. Lazarraga, L. Pascual, J.M. Amarilla, R.M. Rojas, P. Herrero, J.M. Rojo, J. Mater. Chem. 12 (2002) 1184.
[22] M.G. Lazarraga, L. Pascual, H. Gadjov, D. Kovacheva, K. Petrov, J.M. Amarilla, R.M. Rojas, M.A. Martín-Luengo, J.M. Rojo, J. Mater. Chem. 14 (2004) 1640.
[23] L. Pascual, H. Gadjov, D. Kovacheva, K. Petrov, J.M. Amarilla, P. Herrero, R.M. Rojas, J.M. Rojo, J. Electrochem. Soc. 152 (2005) A301.
[24] S.R. Jain, K.C. Adiga, V.R. Pai Verneker, Combust. Flame 40 (1981) 71.
[25] Y. Zhang, G.C. Stangle, J. Mater. Res. 8 (1994) 1997.
[26] J. Laugier, A. Filhol, CelRef, PC Version (unplished) ILL, Grenoble, France, 1991.
[27] M.G. Lazarraga, S. Mandal, J. Ibáñez, J.M. Amarilla, J.M. Rojo, J. Power Sources 115 (2003) 315.
[28] M.D. Judd, B.A. Plunkett, M.I. Pope, J. Thermal Anal. 6 (1974) 555.
[29] L. Patron, O. Carp, I. Mindru, G. Marinescu, E. Segal, J. Thermal Anal. Cal. 72 (2003) 281.
[30] S. Mandal, R.M. Rojas, J.M. Amarilla, P. Calle, N. Kosova, V.F. Anufrienko, J.M. Rojo, Chem. Mater. 14 (2002) 1598.
[31] R.D. Shannon, Acta Crystallogr. A32 (1976) 767.
[32] B. Markovsky, Y. Talyossef, G. Salitra, D. Aurbach, H.-J. Kim, S. Choi, Electrochem. Commun. 6 (2004) 821.
[33] Y. Shin, A. Manthiram, J. Electrochem. Soc. 151 (2004) A204.